

Research on Field Strength Calculation of Antenna Far Field

WANG Wei

Department of Electronic Engineering, Xi'an Aeronautical University, Xi'an Shaanxi 710077, China
weiiwang[at]qq.com

Abstract: In a two-dimensional space, the outline is approximated by a triangular column, and an array antenna is simulated with a set of infinitely long line current sources. The calculation is carried out using the methods of moments (MoM) and the finite element method (FEM) respectively, to analyze the influence on the radiation field of the array antenna in the presence of a conductor nose cone. Experimental results show that, as the rotation angle of the antenna array changes, conductor shielding has a significant impact on the far field strength and deviation angle, especially the nose cone size has a significant effect on the antenna radiation field.

Keywords: Conductor nose cone; array antenna; radiation field

1. Mathematical Model

The nose cone is usually in the shape of a conical rotating body [1] [2], which is mathematically modeled by a two-dimensional infinite triangular column; for an array antenna that rotates mechanically with its own center as the axis, mathematical simulation is performed with a set of equally spaced infinite current sources [3], the mathematical calculation model is shown in Figure 1.

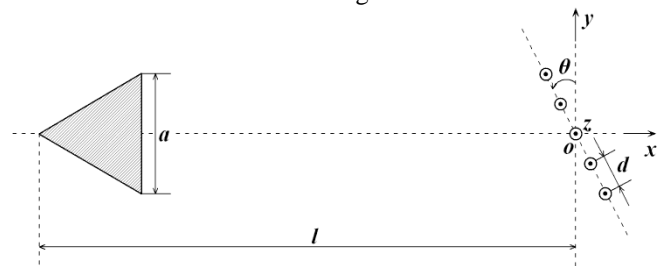


Figure 1: Calculation model

Among them, a represents the cross-sectional side length of the conductor triangular column, l represents the distance between the conductor and the antenna array, the coordinate origin o is the center of the array antenna, d is the antenna element spacing, and θ corresponds to the rotation angle of the antenna.

The research goal of this paper is to solve the electric field of distant points distributed on the arc centered on the origin, and analyze the influence of the far field in the relevant radiation direction. Since the target cylinder and the line current as the excitation source are parallel to the z coordinate axis, the electric field generated by each line current can be expressed as [4],

$$E_z^{inc}(\vec{\rho}) = -I_z \frac{\omega\mu_0}{4} H_0^{(2)}(k_0|\vec{\rho} - \vec{\rho}'|) \quad (1)$$

When using the method of moments to solve, the electric field integral equation of the research target is [5],

$$\frac{\omega\mu_0}{4} \int_c J_z(\vec{\rho}') H_0^{(2)}(k_0|\vec{\rho} - \vec{\rho}'|) dl' = E_z^{inc}(\vec{\rho}) \quad (2)$$

Select the pulse basis function, solve the integral equation by the point matching method [6], obtain the current distribution on the conductor surface, and then calculate the far field [7],

$$E_z^{sca}(\vec{\rho}) = -\frac{\omega\mu_0}{4} \sum_{n=1}^N J_n(\vec{\rho}') \int_{c_n} H_0^{(2)}(k_0|\vec{\rho} - \vec{\rho}'|) dl' \quad (3)$$

When the finite element method [8] is used to solve the problem, the problem can be expressed by Helmholtz equation as,

$$\frac{\partial}{\partial x} \left(\frac{1}{\mu_r} \frac{\partial E_z}{\partial x} \right) + \frac{\partial}{\partial y} \left(\frac{1}{\mu_r} \frac{\partial E_z}{\partial y} \right) + k_0^2 \epsilon_r E_z = 0 \quad (4)$$

Combining the second-order absorbing boundary conditions, using the Ritz method to discretize the corresponding variational formula, the near-field distribution around the conductor is solved, and the far-field expression is:

$$E(\vec{\rho}) = \oint_{\Gamma} \left[E(\vec{\rho}') \frac{\partial G_0(\vec{\rho}, \vec{\rho}')}{\partial n'} - G_0(\vec{\rho}, \vec{\rho}') \frac{\partial E(\vec{\rho}')}{\partial n'} \right] d\Gamma' \quad (5)$$

Where,

$$G_0(\vec{\rho}, \vec{\rho}') = \frac{1}{4j} H_0^{(2)}(k_0|\vec{\rho} - \vec{\rho}'|) \quad (6)$$

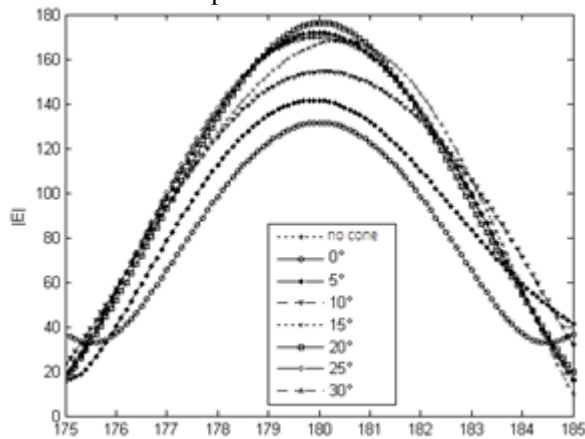
2. Experimental Results and Analysis

During the experiments, set the triangular column side length a to 2λ , the conductor-array distance l to 30λ , the antenna array element spacing d to 0.5λ , and the antenna array rotation angle θ to be within the range of 0 to 30° . The far field is 530λ away from the center of the antenna array.

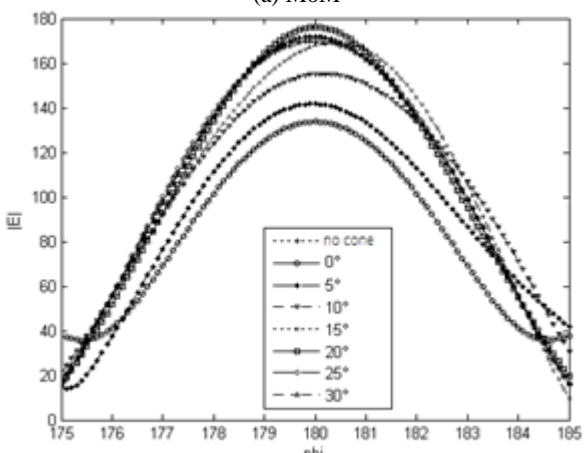
When the array width is 10λ , that is, when 21-unit line current sources are included, the far-field distribution calculated by MoM and FEM are shown in Figure 2. Due to the need to observe the peak direction angle offset the irradiation direction angle, the electric field amplitude curve in Fig. 2 has been shifted moderately, so that $\varphi=180^\circ$ always indicates the direction of the array antenna. It can be seen from the figure that, the calculation results of the two methods are consistent, and both show the changing law of the far field distribution under different rotation angles.

When the conductor is directly in front of the array, the shielding effect is most significant. With the increase of the rotation angle, the field distribution gradually approaches the situation without shielding. At a certain rotation angle, the

presence of conductor shielding even increases the peak value of the electric field amplitude.



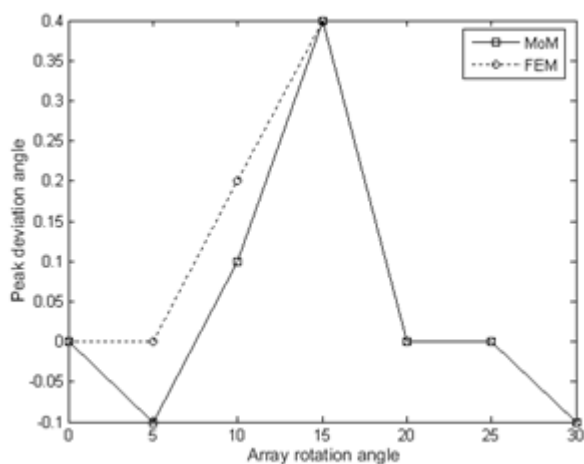
(a) MoM



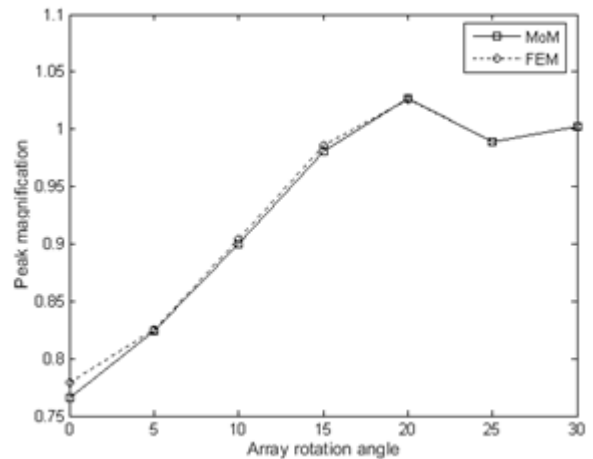
(b) FEM

Figure 2: The distribution of the antenna's far field varies with the rotation angle of the array.

When the array width is 10λ and 15λ , the offset results of the electric field peak value to the incident direction are shown in Figure 3 and Figure 4. It can be found from the figures that, when the array width is small, the influence of conductor shielding on the peak direction and amplitude is more obvious. In both array widths, the peak value is enlarged, which occurs when the rotation is 20° and 25° , respectively. When the maximum peak occurs, the peak direction is always close to the actual array direction.

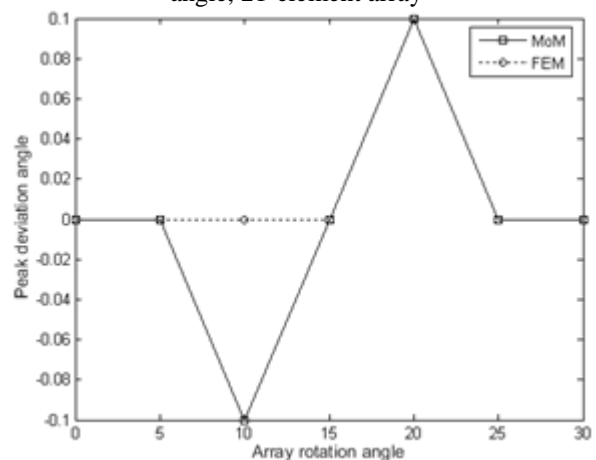


(a) Angle offset

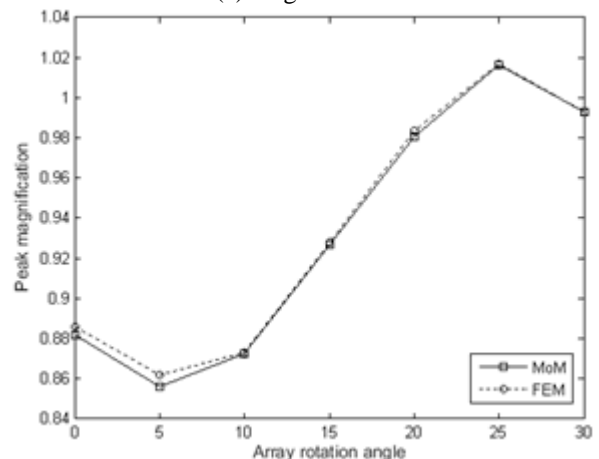


(b) Amplitude change

Figure 3: Variation of far-field peak value with rotation angle, 21-element array



(a) Angle offset



(b) Amplitude change

Figure 4: Variation of far-field peak value with rotation angle, 31-element array

Replace the right straight line boundary of the triangular column conductor section in Figure 1 with an arc boundary. The radius of the arc is 2λ . The center of the arc on the left side of the boundary represents the convex bottom of the nose cone, and the right side means the bottom is concave. The MoM is used to calculate the far-field distribution to analyze the influence of the bottom shape of the nose cone on the array radiation. During the calculation process, the array is not rotated, and the width is 10λ . The calculation result is shown in Figure 5. It can be seen from Figure 5 that, the shape

of the bottom of the nose cone has little effect on the far-field distribution, indicating that the shape of the bottom of the nose cone is not the decisive factor on affecting the antenna radiation effect.

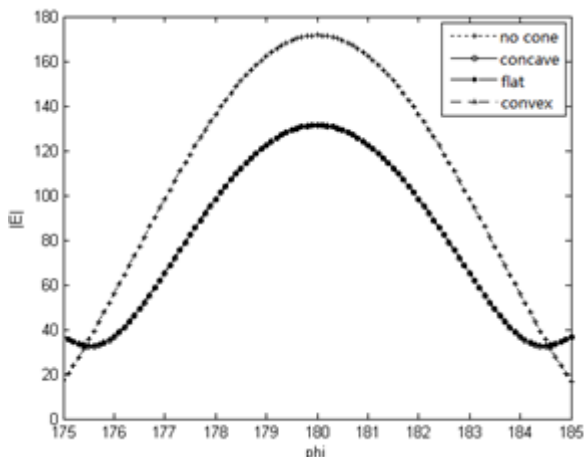


Figure 5: The far-field distribution under the occlusion of the nose cone with different bottom shapes.

Set the side length a of the conductor cross-section in Figure 1 to be in the range of $0.1\lambda \sim 5\lambda$, use an unrotated array with a width of 10λ to illuminate, and use the MoM to calculate the far-field distribution to investigate the influence of the size of the conductor target on the antenna radiation. The far-field distribution is shown in Figure 6. The results in the figure show that the larger the nose cone size, the more significant the occlusion effect.

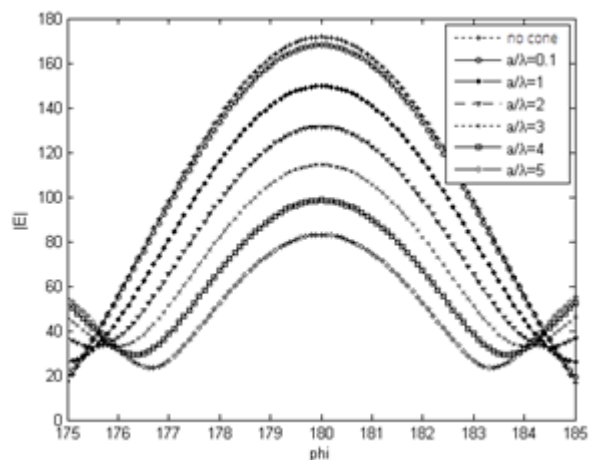


Figure 6: The far-field distribution under the occlusion of different sizes of nose cones

3. Conclusion

In this paper, the influence of the shielding of the conductor target in the near area of the antenna on the radiation characteristics of the antenna is studied. The MoM and the FEM methods are used to calculate the change law of the far field under different array widths. The experimental results show that, as the rotation angle of the antenna array changes, the conductor shielding has a significant impact on the far field strength and deviation angle, and even the radiation field strength is amplified. At the same time, the shape change of the conductor bottom has no obvious effect on the antenna radiation field, while the nose cone size has a significant

effect on the antenna radiation field.

4. Acknowledgements

This work was supported by the National Natural Science Foundation of China (grant number 61901350); Higher Education Research Project of Xi'an Aeronautical University (grant number 2019GJ1006), and Science Research Fund of Xi'an Aeronautics University (grant number 2019KY0208).

References

- [1] E. Whalen, G. Gampala, K. Hunter, S. Mishra and C. J. Reddy, "Aircraft Radome Characterization via Multiphysics Simulation," 2018 AMTA Proceedings, Williamsburg, VA, 2018, pp. 1-4.
- [2] O. I. Sukharevsky, V. A. Vasilets, S. V. Nechitaylo and I. E. Ryapolov, "The radiation characteristics of antenna systems with a cone-sphere radome," 2017 IEEE First Ukraine Conference on Electrical and Computer Engineering (UKRCON), Kiev, 2017, pp. 106-109.
- [3] G. A. E. Crone, A. W. Rudge, G. N. Taylor. Design and Performance of Airborne Radomes: A Review. IEE PROC. , Vol. 128, Pt. F, No. 7. December 1981, pp451~464..
- [4] C. A. Balanis. *Advanced Engineering Electromagnetics*. New York: John Wiley & Sons, 1989.
- [5] C. C. Lu, Calculation and measurement of electromagnetic scattering. Beijing: Beijing University of Aeronautics and Astronautics Press, 2006.
- [6] C. C. Lu, "A fast algorithm based on volume integral equation for analysis of arbitrarily shaped dielectric radomes," in IEEE Transactions on Antennas and Propagation, vol. 51, no. 3, pp. 606-612, March 2003.
- [7] O. I. Sukharevsky and V. A. Vasilets, "Scattering of MiG-29 antenna with dielectric radome," 2013 IX International Conference on Antenna Theory and Techniques, Odessa, 2013.
- [8] J. M. Jin, The Finite Element Method in Electromagnetics. 2nd ed. New York: John Wiley & Sons, 2002.

Author Profile



WANG Wei received the B.E. degree in electronics and information technology, the Master's degree in aerospace propulsion theory and engineering and the Ph.D. degree in electronic science and technology from the Northwestern Polytechnical University, Xi'an, China. Since 2015, he has been a lecturer in Xi'an Aeronautics University. His current research interests include antenna and radome design, electromagnetic scattering analysis and intelligent optimization algorithm.